Available online at www.sciencedirect.com

ScienceDirect

Ceramics International 40 (2014) 2593–2598

CERAMICS INTERNATIONAL

www.elsevier.com/locate/ceramint

# Effects of excess boron on combustion synthesis of alumina–tantalum boride composites

C.L. Yeh*, Y.S. Huang

*Department of Aerospace and Systems Engineering, Feng Chia University, 100 Wenhwa Rd., Seatwen, Taichung 40724, Taiwan*

Received 2 August 2013; received in revised form 11 October 2013; accepted 17 October 2013
Available online 25 October 2013

**Abstract**

TaB- and $TaB_2$–$Al_2O_3$ in situ composites were fabricated by thermite-incorporated combustion synthesis from the powder mixtures of different combinations, including $Ta_2O_5$–Al–B, $Ta_2O_5$–Al–$B_2O_3$–B, and $Ta_2O_5$–$B_2O_3$–Al. Effects of excess boron were studied on the combustion dynamics and phase constituents of final products. For the $B_2O_3$-containing samples, the reaction was less exothermic and aluminothermic reduction of $Ta_2O_5$ and $B_2O_3$ was less complete, resulting in the deficiency of boron and the presence of $TaO_2$ and Ta. For the samples containing elemental boron, the occurrence of borothermic reduction of $Ta_2O_5$ also caused the loss of boron. Experimental evidence showed that boron in excess of the stoichiometric amount substantially enhanced the formation of tantalum borides, which in turn facilitated the reduction of $Ta_2O_5$ by Al. Consequently, the samples rich with boron in the molar proportions of $Ta_2O_5$:Al:B = 3:10:9 and 3:10:16 (i.e., B/Ta = 1.5 and 2.67) were found to be the optimum stoichiometries of producing TaB- and $TaB_2$–$Al_2O_3$ composites through a self-sustaining combustion process.


*Keywords:* A. Powders: solid state reaction; B. X-ray methods; D. $Al_2O_3$; D. Borides; Combustion synthesis

## 1. Introduction

Transition metal (Groups IVb and Vb) borides, such as $TiB_2$, $ZrB_2$, $HfB_2$, $TaB_2$, etc., have attracted great attention because of their unique combination of many favorable properties, including high melting temperatures, high hardness, good chemical stability, high electrical and thermal conductivity, and good wear and corrosion resistance [1–3]. The combination of properties makes these materials potential candidates for a variety of high-temperature applications, including engines, rocket motor nozzles, plasma arc electrodes, cutting tools, ballistic armors, and furnace elements [4]. Moreover, many reinforcing additives such as $Al_2O_3$ [5,6], $ZrO_2$ [7], TiC [8], and SiC [9,10] have been incorporated to improve the mechanical properties of various transition metal borides and carbides.

For the formation of high temperature materials, combustion and plasma synthesis are two important fabrication routes [11–13]. Combustion synthesis, particularly in the mode of self-propagating high-temperature synthesis (SHS), takes advantage of the intense energy release from highly exothermic reactions, and hence, has the merits of high energy efficiency, simplicity, high productivity, structural and functional diversity of final products, etc. [14,15]. Furthermore, combustion synthesis involving aluminothermic reduction of metal oxides (i.e., the thermite reaction) represents an in situ technique for producing composite materials with the addition of $Al_2O_3$ [16,17]. Considerable exothermicity of the thermite reaction is beneficial for the SHS process, and the use of metal oxides as the starting materials instead of metallic elements is often cost-effective [18,19].

In view of the extremely high melting temperatures above 3000 °C for tantalum borides (TaB and $TaB_2$), composite materials based on TaB and/or $TaB_2$ are particularly promising for the ultra high-temperature applications. Although the formation of tantalum borides by SHS is feasible from the elemental powder compacts [20], both reagents are rather costly. Therefore, it is worthwhile to employ less expensive $Ta_2O_5$ and $B_2O_3$ as reactants in a thermite-based SHS process for the formation of TaB- and $TaB_2$–$Al_2O_3$ in situ composites.

*Corresponding author. Tel.: +886 4 2451 7250x3963; fax: +886 4 2451 0862.
*E-mail address:* clyeh@fcu.edu.tw (C.L. Yeh).

0272-8842/$ - see front matter © 2013 Elsevier Ltd and Techna Group S.r.l. All rights reserved.
http://dx.doi.org/10.1016/j.ceramint.2013.10.082

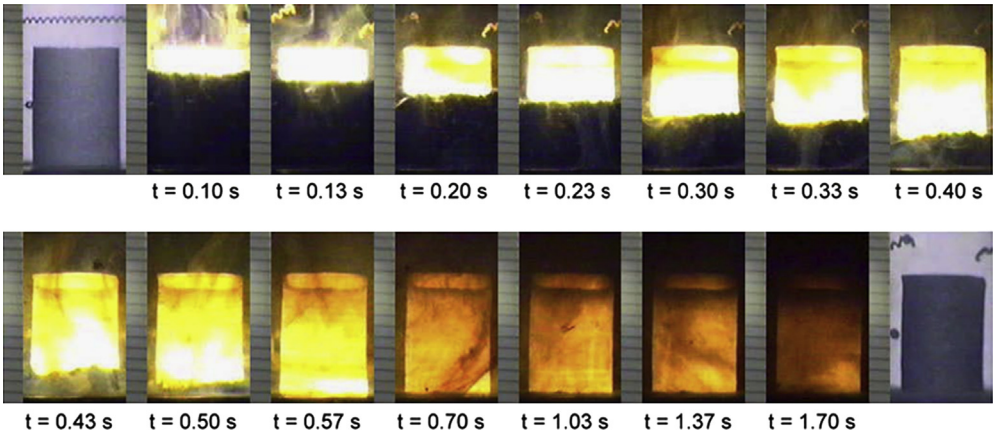


Fig. 1. Recorded SHS sequences illustrating self-sustaining combustion along a powder compact of $3Ta_2O_5+10Al+xB$ with $x=15$.

In order to resolve the boron-deficient problem [21,22], the samples with excess boron were conducted in this study. Moreover, the effects of excess boron on the combustion temperature, reaction front velocity, and boride phases formed in the final products are investigated.

## 2. Experimental methods of approach

The starting powders adopted by this study included $Ta_2O_5$ (Strem Chemicals, 99.9%), $B_2O_3$ (Strem Chemicals, 99.9%), Al (Showa Chemical Co., $<45$ μm, 99.9%), and amorphous boron (Noah Technologies Corp., $<1$ μm, 92% purity). The first type of the reaction system expressed in Reactions (1) and (2) was designed to contain amorphous boron and to study the effect of excess boron.

$$3Ta_2O_5+10Al+xB\rightarrow 6TaB/TaB_2+5Al_2O_3, \quad \text{with } x=6\text{–}16 \tag{1}$$

$$3Ta_2O_5+12Al+B_2O_3+yB\rightarrow 6TaB/TaB_2+6Al_2O_3, \quad \text{with } y=4\text{–}14 \tag{2}$$

The reactant mixture of Reaction (1) comprises $Ta_2O_5$, Al, and B powders under a molar proportion of $3Ta_2O_5+10Al+xB$ with $x=6$–16. In Reaction (1), aluminothermic reduction of $Ta_2O_5$ produces Ta and $Al_2O_3$, and the reduced Ta reacts subsequently with boron. As the parameter $x$ exceeds the stoichiometric values for the synthesis of TaB and $TaB_2$ (i.e., $x=6$ and 12, respectively), the SHS process is considered to proceed with excess boron.

Reaction (2) employs two oxide reagents, $Ta_2O_5$ and $B_2O_3$, to mix with Al and boron in the composition of $3Ta_2O_5+12Al+B_2O_3+yB$ with $y=4$–14. The role of $B_2O_3$ in Reaction (2) is the other source of boron. That is, co-reduction of $Ta_2O_5$ and $B_2O_3$ by Al is required. Similar to Reaction (1), the effect of excess boron is studied by Reaction (2), where $y=4$ signifies the exact stoichiometric condition for the formation of TaB and $y=10$ for that of $TaB_2$.

The second type of the reactant mixture is free of amorphous boron and adopts $B_2O_3$ as the only supply of boron. Reactions (3) and (4) are intended to produce TaB- and $TaB_2$–$Al_2O_3$ composites, respectively, from the mixtures of $Ta_2O_5$, $B_2O_3$, and Al powders.

$$3Ta_2O_5+3B_2O_3+16Al\rightarrow 6TaB+8Al_2O_3 \tag{3}$$

$$3Ta_2O_5+6B_2O_3+22Al\rightarrow 6TaB_2+11Al_2O_3 \tag{4}$$

The reactant powders with designed compositions were dry mixed in a ball mill and then cold-pressed into the cylindrical samples with a diameter of 7 mm, a height of 12 mm, and a compaction density of 50% relative to the theoretical maximum density (TMD). The SHS experiment was conducted in a stainless-steel windowed chamber under an atmosphere of high purity argon (99.99%). Details of the experimental setup and measurement approach were previously reported [23]. In addition, Vickers hardness ($H_v$) and fracture toughness ($K_{IC}$) of the synthesized composites were evaluated [24].

## 3. Results and discussion

### 3.1. Measurement of flame-front propagation velocity

Fig. 1 shows a typical combustion process recorded from Reaction (1) with $x=15$. It is evident that a distinct combustion front forms upon ignition and propagates along the sample in a self-sustaining manner. As clearly revealed in Fig. 1, the progression of the combustion wave is accompanied with visible smoke, implicative of the formation of gaseous products or an aerosol of solid or liquid particulates. It is believed that a certain degree of borothermic reduction of $Ta_2O_5$ occurred and led to the yield of gaseous BO and molten $B_2O_3$, both of which were then expelled from the porous sample. This was subsequently responsible for the lack of boron to form tantalum borides.

The propagation velocity ($V_f$) of the combustion front was determined from the recorded SHS images. As presented in Fig. 2, the flame-front velocity is affected not only by the atomic ratio of B/Ta of the reactant mixture, but also by the use of $B_2O_3$ as the reagent. With the increase of the boron content of Reaction (1) from B/Ta=1.0 to 2.67 (i.e., $x=6$–16), the combustion wave velocity increases from 16.1 mm/s to a peak

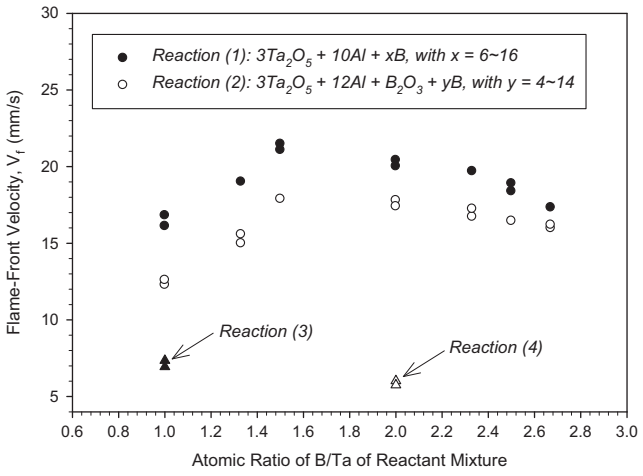


Fig. 2. Effect of atomic ratio of B/Ta on flame-front propagation velocity of powder compacts based upon Reactions (1)–(4).

value of 21.5 mm/s at B/Ta=1.5 ($x$=9), and then decreases to about 18.4 mm/s for the compact with B/Ta=2.67. The composition dependence of the combustion velocity is generally influenced by the reaction exothermicity. The exothermicity of combustion synthesis could be complicated by different boride phases formed in the final products, completeness of metallothermic reduction, and the amount of extra boron.

The variation of the flame-front velocity of Reaction (2) with the atomic ratio of B/Ta is the same as that of Reaction (1). Due most likely to the weaker reaction exothermicity of the $B_2O_3$-containing sample, however, the flame speed of Reaction (2) is lower than that of Reaction (1). The reaction heats liberated per one mole of $Al_2O_3$ formed from aluminothermic reduction of $B_2O_3$ and $Ta_2O_5$ are 403.8 and 448.1 kJ [25], respectively. Moreover, the partial reduction of $B_2O_3$ tends to produce BO gases and the ejection of BO from the sample causes an additional waste of boron. Consequently, a decelerated combustion wave was observed when $B_2O_3$ substituted for amorphous boron in the reactant mixture. The decrease of combustion velocity became more significant for Reactions (3) and (4), since both of them utilized $B_2O_3$ as the single source of boron. According to Fig. 2, the flame-front velocities of Reactions (3) and (4) are about 7.1 and 5.9 mm/s, respectively.

### 3.2. Measurement of combustion temperature

Four combustion temperature profiles measured from the powder compacts of Reaction (1) with different contents of amorphous boron are depicted in Fig. 3(a), where the abrupt rise represents the rapid arrival of the combustion wave and the peak value signifies the reaction front temperature. Fig. 3(a) indicates that the combustion front temperature increases from 1522 to 1690 °C with increasing B/Ta ratio from 1.0 ($x$=6) to 1.5 ($x$=9), followed by a gradual decline to 1551 °C as the amount of boron augments to $x$=16. Based upon the composition analysis of final products to be presented later, the increase of the combustion front temperature with the boron

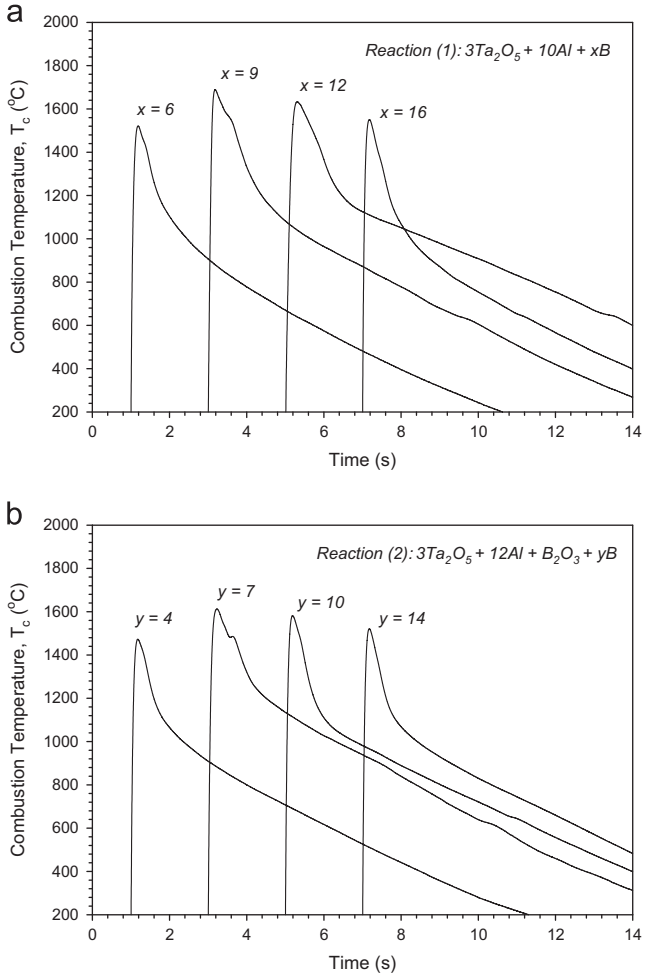


Fig. 3. Effect of boron content on combustion temperature of powder compacts of (a) Reaction (1) and (b) Reaction (2).

content between $x$=6 and 9 is attributed to the improved aluminothermic reduction of $Ta_2O_5$ and the enhanced formation of TaB. The subsequent decrease of the reaction temperature is mainly caused by the change in the boride phases formed in the final products. With the increase of amorphous boron from $x$=12 to 16, the synthesized boride was transformed from a mixture of $TaB_2$ and TaB to single-phase $TaB_2$. That is, TaB was fully converted into $TaB_2$ by the additional boron. According to the previous study on combustion synthesis of the Ta–B compounds [20], the formation of $TaB_2$ was found to be less energetic than that of TaB. This explains the decline of the combustion temperature of Reaction (1) with increasing boron content from $x$=12 to 16.

For the powder compacts of Reaction (2), Fig. 3(b) shows an increase followed by a decrease in the combustion temperature as the amount of amorphous boron augments. Similar to Reaction (1), the highest combustion front temperature of Reaction (2) was detected from the sample with B/Ta=1.5 ($y$=7), which produced the largest amount of TaB among all samples. Due to the inclusion of $B_2O_3$, the combustion temperature of Reaction (2) ranging between 1473 and 1613 °C is lower than that of Reaction (1). It is useful to note that the combustion front temperatures of about 1415 and

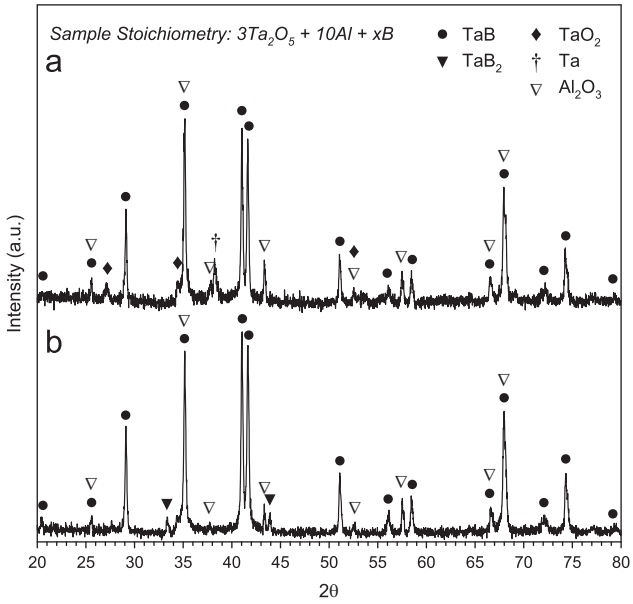


Fig. 4. XRD patterns of products synthesized from samples based on Reaction (1) of $3Ta_2O_5+10Al+xB$ with (a) $x=6$ and (b) $x=9$.

1390 °C were measured from Reactions (3) and (4), respectively. The relatively low reaction temperatures of Reactions (3) and (4) are consistent with their low flame propagation speeds.

### 3.3. Phase constituents of synthesized products

Fig. 4(a) and (b) presents two XRD patterns of the products synthesized from the samples of Reaction (1) with $x=6$ and 9, respectively. A summary of the phase constituents of final products with respect to their initial stoichiometries is compiled in Table 1 for Reactions (1)–(4). As depicted in Fig. 4(a), $TaO_2$ and Ta were identified along with TaB and $Al_2O_3$. The presence of $TaO_2$ signifies incomplete reduction of $Ta_2O_5$ and the unreacted Ta is suggestive of the deficiency of boron. The loss of boron in the forms of BO and $B_2O_3$ from borothermic reduction of $Ta_2O_5$ was proposed earlier. When the amount of boron increased, the remnant Ta was reduced and the yield of TaB was enhanced. The improved formation of TaB intensified combustion exothermicity, and therefore, facilitated aluminothermic reduction of $Ta_2O_5$. As a result, complete reduction of $Ta_2O_5$ was achieved in the sample of $x$=8. The stoichiometry with sufficient boron is verified by Fig. 4(b), indicative of the formation of a TaB–$Al_2O_3$ composite with trivial $TaB_2$ from a powder mixture of B/Ta=1.5 ($x=9$).

For the synthesis of the $TaB_2$–$Al_2O_3$ composite, Fig. 5(a) reveals the detection of three boride phases, $TaB_2$, TaB, and $Ta_3B_4$, along with $Al_2O_3$ from the product of Reaction (1) with $x=12$ (i.e., B/Ta=2.0). The existence of TaB and $Ta_3B_4$ implies lack of boron for complete formation of $TaB_2$. The additional boron was to convert both TaB and $Ta_3B_4$ into $TaB_2$. As reported in Table 1, $Ta_3B_4$ was no longer present in the final product from the sample with boron of $x=15$. When the boron content arrives at $x=16$ (B/Ta=2.67) in Reaction

Table 1
Summary of the phase composition of synthesized products with respect to their initial stoichiometries of Reactions (1)–(4).

| Reaction/ parameter | Phase composition of synthesized products | | | |
|---|---|---|---|---|
| | Dominant boride | Secondary boride (s) | Oxide(s) | Others |
| (1)/$x=6$ | TaB | | $Al_2O_3$, $TaO_2$ | Ta |
| (1)/$x=8$ | TaB | | $Al_2O_3$ | Ta |
| (1)/$x=9$ | TaB | $TaB_2$ | $Al_2O_3$ | |
| (1)/$x=12$, 14 | $TaB_2$ | TaB, $Ta_3B_4$ | $Al_2O_3$ | |
| (1)/$x=15$ | $TaB_2$ | TaB | $Al_2O_3$ | |
| (1)/$x=16$ | $TaB_2$ | | $Al_2O_3$ | |
| (2)/$y=4$–7 | TaB | | $Al_2O_3$, $TaO_2$ | Ta |
| (2)/$y=10$–14 | $TaB_2$ | TaB, $Ta_3B_4$ | $Al_2O_3$ | |
| (3) | TaB | | $Al_2O_3$, $TaO_2$ | Ta |
| (4) | $TaB_2$ | TaB, $Ta_3B_4$ | $Al_2O_3$, $TaO_2$ | Ta |

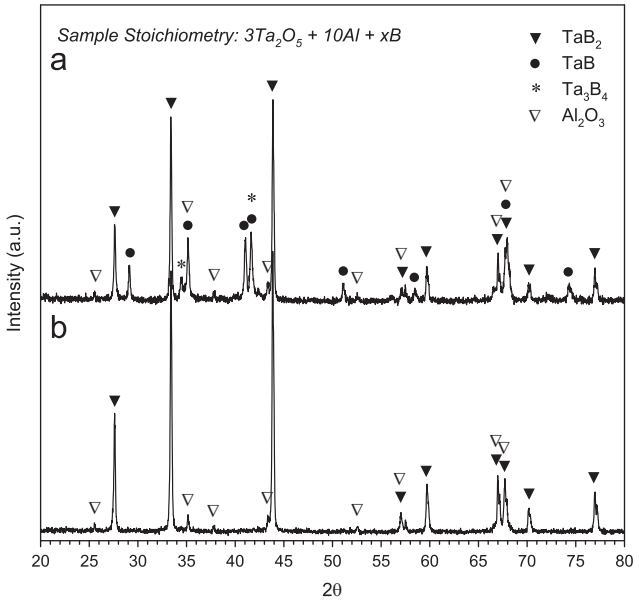


Fig. 5. XRD patterns of products synthesized from samples based on Reaction (1) of $3Ta_2O_5+10Al+xB$ with (a) $x=12$ and (b) $x=16$.

(1), Fig. 5(b) shows the production of a composite containing no more than $TaB_2$ and $Al_2O_3$.

As far as Reaction (2) is concerned, Fig. 6(a) and (b) suggests that the samples of $y=4$ and 7 were subjected to incomplete reduction of $Ta_2O_5$ and lack of boron. Although the increase of boron reduced the amounts of $TaO_2$ and Ta, the effect of excess boron on Reaction (2) was less satisfactory than that on Reaction (1). This could be partly caused by the lower combustion temperature for the $B_2O_3$-containing sample. In part, this might be due to an additional loss of boron stemming from the yield of BO from partial reduction of $B_2O_3$. Therefore, as summarized in Table 1, $TaO_2$ and unreacted Ta are always present along with TaB and $Al_2O_3$ in the final products of Reaction (2) with $y=4$–7 (i.e., B/Ta=1.0–1.5).

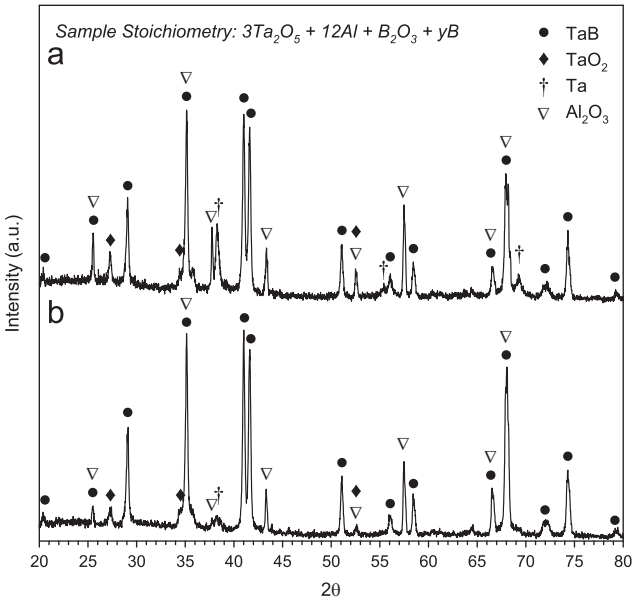


Fig. 6. XRD patterns of products synthesized from samples based on Reaction (2) of $3Ta_2O_5+12Al+B_2O_3+yB$ with (a) $y=4$ and (b) $y=7$.

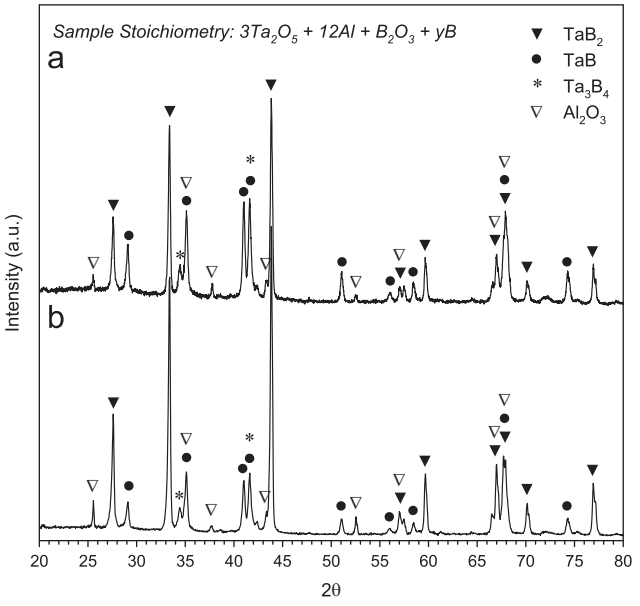


Fig. 7. XRD patterns of products synthesized from samples based on Reaction (2) of $3Ta_2O_5+12Al+B_2O_3+yB$ with (a) $y=12$ and (b) $y=14$.

Two XRD spectra of the final products of Reaction (2) with B/Ta > 2.0 are plotted in Fig. 7(a) and (b), showing three boride phases, $TaB_2$, TaB, and $Ta_3B_4$, even in the case of B/Ta = 2.67 ($y=14$). This means that in order to produce a $TaB_2$–$Al_2O_3$ composite from Reaction (2), the increase of boron to B/Ta = 2.67 did not compensate fully for the lack of boron. Namely, the $B_2O_3$-added sample suffers a larger extent of boron loss.

Similar to Reaction (2), Reactions (3) and (4) involve co-reduction of $Ta_2O_5$ and $B_2O_3$. Due to the larger quantity of $B_2O_3$, however, the reduction of both oxides was less complete for Reactions (3) and (4) than Reaction (2). Therefore, there were relatively great amounts of $TaO_2$ and Ta remaining in the final product of Reaction (3). The product of Reaction (4) was a mixture of many phases including $TaB_2$, TaB, $Ta_3B_4$, $Al_2O_3$, $TaO_2$, and Ta.

Based upon the above composition analysis of SHS-derived products, the most favorable molar proportions for powder compacts to fabricate TaB- and $TaB_2$–$Al_2O_3$ composites are $Ta_2O_5$:Al:B = 3:10:9 and 3:10:16, respectively. The extra amount of boron compensated for the loss of boron largely in the form of gaseous BO. It is instructive to discuss the influence of experimental parameters, including the sample diameter, sample porosity, and pressure of argon, on the optimum starting stoichiometries suggested by this study. Ejection of BO gas from the porous sample is essentially driven by the gas pressure within the pores of the powder compact. Because of the fast reaction rate and high combustion temperature above 1500 °C, the pressure of BO gas in the tiny voids of the sample is considered to be much higher than the argon pressure of about 0.136 MPa. If the initial argon pressure increases, the local pressure inside the pore space will still be higher than the surrounding pressure due to a significant increase in the sample temperature.

As far as the sample porosity is concerned, the practical range of compaction density for the powder compact is between 40% and 70% relative to the theoretical density. The high-temperature CO gas yielded from combustion is readily expelled from the sample of such porosities. For the specimens made up of compressed powders, both the solid matrix and the pore space are often continuous. The pore network is accessible for gas to flow. Therefore, the increase of sample diameter will not prevent CO gas from being ejected. The above argument confirms the optimum proportions of the reagents for SHS formation of TaB- and $TaB_2$–$Al_2O_3$ composites.

Vickers hardness of the TaB–$Al_2O_3$ composite synthesized from Reaction (1) of $x=9$ is approximately 17.8 GPa and the fracture toughness is about 4.1 MPa $m^{1/2}$. For the $TaB_2$–$Al_2O_3$ composite obtained from Reaction (1) of $x=16$, the hardness and fracture toughness are 18.1 GPa and 4.3 MPa $m^{1/2}$, respectively.

## 4. Conclusions

Combustion synthesis involving aluminothermic reduction of $Ta_2O_5$ and $B_2O_3$ was conducted to fabricate TaB- and $TaB_2$–$Al_2O_3$ in situ composites. Besides $B_2O_3$, amorphous boron was adopted as the source of boron and the amount of boron required to make up for the loss of boron during the SHS process was determined. Reactant mixtures for the sample compacts were prepared in the following combinations: $3Ta_2O_5+10Al+xB$ with $x=6$–16, $3Ta_2O_5+12Al+B_2O_3+yB$ with $y=4$–14, $3Ta_2O_5+3B_2O_3+16Al$, and $3Ta_2O_5+6B_2O_3+22Al$. Their combustion behavior and product composition were investigated.

For the samples containing elemental boron, a certain degree of borothermic reduction of $Ta_2O_5$ could occur during combustion and caused the lack of boron to react fully with Ta.

For the $B_2O_3$-containing samples, partial reduction of $B_2O_3$ represented another path of losing boron. Moreover, relatively weak exothermicity of the $B_2O_3$-containing sample hindered $Ta_2O_5$ from being totally reduced. As a result, the highest combustion exothermicity and the most favorable product were obtained from the powder compact composed of $Ta_2O_5$, Al, and boron. For the samples of $3Ta_2O_5+10Al+xB$, the combustion temperature and flame-front velocity increased with boron content from $x=6$ to 9, due to the improved formation of TaB. A decrease in both combustion temperature and velocity was observed for the samples with boron from $x=12$ to 16, because the boride phase formed was converted from a TaB–$TaB_2$ mixture to monolithic $TaB_2$. The effect of excess boron was substantiated by formation of the TaB and $TaB_2$–$Al_2O_3$ composites from the boron-rich samples of $3Ta_2O_5+10Al+xB$ with $x=9$ and 16 (i.e., B/Ta=1.5 and 2.67), respectively.

## Acknowledgments

This research was sponsored by the National Science Council of Taiwan, ROC, under the Grants of NSC 100-2221-E-035-074-MY2. Authors express their gratitude to the Precision Instrument Support Center of Feng Chia University for providing the measurement facilities.

## References

[1] R. Königshofer, S. Fürnsinn, P. Steinkellner, W. Lengauer, R. Haas, K. Rabitsch, M. Scheerer, Solid-state properties of hot-pressed $TiB_2$ ceramics, Int. J. Refract. Met. Hard Mater. 23 (2005) 350–357.

[2] W.G. Fahrenholtz, G.E. Hilmas, I.G. Talmy, J.A. Zaykoski, Refractory diborides of zirconium and hafnium, J. Am. Ceram. Soc. 90 (2007) 1347–1364.

[3] X. Zhang, G.E. Hilmas, W.G. Fahrenholtz, Synthesis, densification, and mechanical properties of $TaB_2$, Mater. Lett. 62 (2008) 4251–4253.

[4] E. Wuchina, E. Opila, M. Opeka, W. Fahrenholtz, I. Talmy, UHTCs: ultra-high temperature ceramic materials for extreme environment applications, Electrochem. Soc. Interface 16 (2007) 30–36.

[5] M. Gu, C. Huang, S. Xiao, H. Liu, Improvements in mechanical properties of $TiB_2$ ceramics tool materials by dispersion of $Al_2O_3$ particles, Mater. Sci. Eng. A 486 (2008) 167–170.

[6] J. Zhu, R. Pan, Synthesis and mechanical properties of (Ti, $Mo)_2AlC$/$Al_2O_3$ composite by a reaction hot pressing method, Ceram. Int. 39 (2013) 5609–5613.

[7] X. Zhang, W. Li, C. Hong, W. Han, Microstructure and mechanical properties of $ZrB_2$-based composites reinforced and toughened by zirconia, Int. J. Appl. Ceram. Technol. 5 (2008) 499–504.

[8] S.K. Bhaumik, C. Divakar, A.K. Singh, G.S. Upadhyaya, Synthesis and sintering of $TiB_2$ and $TiB_2$–TiC composite under high pressure, Mater. Sci. Eng. A 279 (2000) 275–281.

[9] R. Licheri, R. Orrù, C. Musa, G. Cao, Synthesis, densification and characterization of $TaB_2$–SiC composites, Ceram. Int. 36 (2010) 937–941.

[10] A. Ortona, P. Fino, C. D'Angelo, S. Biamino, G. D'Amico, D. Gaia, S. Gianella, Si–SiC–$ZrB_2$ ceramics by silicon reactive infiltration, Ceram. Int. 38 (2012) 3243–3250.

[11] Z.A. Munir, J.B. Holt (Eds.), Combustion and Plasma Synthesis of High Temperature Materials, VCH, New York, 1990.

[12] A. Orlov, J. Grabis, Plasma chemical synthesis of fine $MoSi_2$ and $MoSi_2$–$Si_3N_4$ composite powders, High Temp. Mat. Proc 15 (2011) 299–306.

[13] Z.G. Kostic, P.Lj. Stefanovic, P.B. Pavlovic, D.B. Cvetinovic, Possibility of composite silicon nitride+silicon carbide ($Si_3N_4$SiC) powder production in thermal plasma, High Temp. Mat. Proc. 15 (2011) 321–328.

[14] A.G. Merzhanov, Combustion and explosion processes in physical chemistry and technology of inorganic materials, Russ. Chem. Rev 72 (2003) 289–310.

[15] G. Liu, J. Li, K. Chen, Combustion synthesis of refractory and hard materials: a review, Int. J. Refract. Met. Hard Mater. 39 (2013) 90–102.

[16] S.E. Aghili, M.H. Enayati, F. Karimzadeh, In-situ synthesis of alumina reinforced $(Fe,Cr)_3Al$ intermetallic matrix nanocomposite, Mater. Manuf. Process. 27 (2012) 1348–1353.

[17] L.L. Wang, Z.A. Munir, Y.M. Maximov, Thermite reactions: their utilization in the synthesis and processing of materials, J. Mater. Sci. 28 (1993) 3693–3708.

[18] C.L. Yeh, Y.S. Huang, Thermite reduction of $Ta_2O_5$/$SiO_2$ powder mixtures for combustion synthesis of Ta-based silicides, J. Alloys Compd. 509 (2011) 6302–6306.

[19] C.L. Yeh, Y.S. Huang, Thermite-based combustion synthesis of niobium silicides/$Al_2O_3$ composites, High Temp. Mat. Proc. 16 (2012) 57–69.

[20] C.L. Yeh, H.J. Wang, A comparative study on combustion synthesis of Ta–B compounds, Ceram. Int. 37 (2011) 1569–1573.

[21] P. Peshev, G. Bliznakov, L. Leyarovska, On the preparation of some chromium, molybdenum and tungsten Borides, J. Less-Common Met. 13 (1967) 241–247.

[22] C.L. Yeh, J.Z. Lin, H.J. Wang, Formation of chromium borides by combustion synthesis involving borothermic and aluminothermic reduction of $Cr_2O_3$, Ceram. Int. 38 (2012) 5691–5697.

[23] C.L. Yeh, J.Z. Lin, Combustion synthesis of Cr–Al and Cr–Si intermetallics with $Al_2O_3$ additions from $Cr_2O_3$–Al and $Cr_2O_3$–Al–Si reaction systems, Intermetallics 33 (2013) 126–133.

[24] C.L. Yeh, W.J. Yang, Formation of MAX solid solutions $(Ti,V)_2AlC$ and $(Cr,V)_2AlC$ with $Al_2O_3$ addition by SHS involving aluminothermic reduction, Ceram. Int. 39 (2013) 7537–7544.

[25] M. Binnewies, E. Milke, Thermochemical Data of Elements and Compounds, Wiley-VCH Verlag GmbH, Weinheim, New York, 2002.